RETRIEVING AEROSOL CHARACTERISTICS FROM SATELLITE OCEAN COLOR MULTI-SPECTRAL SENSORS USING A NEURAL-VARIATIONAL METHOD

D. Diouf[1], S. Thiria[2], A. Niang[1], J. Brajard[2] and M. Crepon[2]
[1]*Ecole Supérieure Polytechnique, Université Cheikh Anta Diop de Dakar, BP 5085, Dakar Fann, Sénégal*
[2]*IPSL/LOCEAN, Université Paris 6, 75252, Paris, France*

Keywords: Multi-layer perceptrons, Atmospheric correction, Variational inversion.

Abstract: We present a new algorithm suitable for retrieving and monitoring Saharan dusts from satellite ocean-color multi-spectral observations. This algorithm comprises two steps. The first step consists in classifying the TOA spectra using a neuronal classifier, which provides the aerosol type and a first guess value of the aerosol parameters. The second step retrieves accurate aerosol parameters by using a variational optimization method. We have analyzed 13 years of SeaWiFS images (September 1997-December 2009) in an Atlantic Ocean area off the coast of West Africa. As the method takes into account Saharan dusts, the number of pixels processed is an order of magnitude higher than that processed by the standard SeaWiFS algorithm. We note a strong seasonal variability. The Saharan dust concentration is maximal in summer during the rainy season and minimal in autumn when the vegetation bloom due to the rainy season prevents soil erosion by the wind.

1 INTRODUCTION

Aerosols are an important component of the Earth climate system. They reflect the downwelling solar radiations and thus contribute to cooling the atmosphere on the one hand and on the other hand, they may also absorb infrared radiation emitted by Earth, thus contributing to warming the atmosphere depending on their quality. A good knowledge of aerosol properties is therefore necessary for understanding climate variability and modeling it. The mass concentration of aerosols is closely related to the optical thickness τ, which is a measure of the light attenuation. Aerosols are also characterized by their type (dust, maritime, soot ...).

A major source of aerosols is the Sahara desert, which seeds the tropical Atlantic atmosphere with

Saharan dusts, which are absorbing aerosols. These aerosols cross the Atlantic Ocean transported by the trades winds and may be detected as far away as the Caribbean Island and South America (Moulin et al, 1997).

During the last 15 years, several satellites carrying multi-spectral radiometers dedicated to ocean-color observation have been launched. They provide a daily global coverage of Earth at a scale of some kilometers. These ocean-color radiometers also provide information about aerosol parameters, since the atmosphere is located between the ocean and the satellite. Ocean color radiometer signals have been intensively used to monitor aerosol parameters over the ocean (Gordon and Wang, 1994); (Tanré et al., 1997) and to retrieve their most significant parameters.

The standard aerosol products provided by Space Agencies such as the SeaWiFS products distributed by NASA are limited to a quite low optical thickness (less than 0.35). Moreover, the algorithms used for SeaWiFS products are not able to deal with absorbing aerosols nor to retrieve the aerosol typology.

This paper presents a new method for deriving aerosol characteristics including those of absorbing aerosols, from satellite ocean-color data.

2 DATA SETS

2.1 The SeaWiFS Data Set

For this study we use daily luminance measurements made by the SeaWiFS sensor off the West Africa

Diouf D., Thiria S., Niang A., Brajard J. and Crepon M..
RETRIEVING AEROSOL CHARACTERISTICS FROM SATELLITE OCEAN COLOR MULTI-SPECTRAL SENSORS USING A NEURAL-VARIATIONAL METHOD.
DOI: 10.5220/0003638802970303
In *Proceedings of the International Conference on Neural Computation Theory and Applications* (NCTA-2011), pages 297-303
ISBN: 978-989-8425-84-3
Copyright © 2011 SCITEPRESS (Science and Technology Publications, Lda.)

coast in an area between 8°-24°N and 14°-30°W. These measures extend the period of 1997-2009. Luminances are at wavelengths 412nm, 443nm, 490nm, 510nm, 555nm, 670nm.765nm and 865nm. For each wavelength λ, the TOA reflectance ρ is computed.

According to Gordon and Wang (1994) the Top Of the Atmosphere (TOA) reflectance ρ is the sum of several components that can be computed separately: the Rayleigh multiple scattering (air molecules) in the absence of aerosols, can be accurately computed by using the atmospheric pressure, and the whitecap contribution by taking into account the wind speed. We removed pixels contaminated by the sun glitter, using a geometrical mask. The signal that was finally used in our classification method was therefore:

$$\rho_{used} = \rho_a + \rho_{ra} + t\rho_w \quad (1)$$

where ρ_a is the reflectance resulting from multiple scattering of aerosols in the absence of the air, ρ_{ra} is the interaction term between molecular and aerosol scattering, ρ_w, is the contribution of the water and t is the transmittance of the atmosphere at a given wavelength (λ).

In equation (1), ρ_w is small in the red and near-infrared, so that ρ_{used} mainly depends on the aerosol term $\rho_a+\rho_{ra}$ at 670, 765 and 865 nm. For the other visible bands, it is expected that the aerosol term remains large enough in most situations to allow us to retrieve pertinent information (in particular absorption capability) about the particles at these wavelengths.

We used satellite data sets comprising ten dimensional vectors, whose components are eight wavelengths measured by the radiometer and two viewing angles since the reflectance spectra depend on the geometry of the measurement. These angles are the sun zenith angle θ_s and the scattering angle γ defined as:

$$\gamma = \arccos\left(-\cos\theta_v \cos\theta_s + \sin\theta_v \sin\theta_s \cos\Delta\Phi\right) \quad (2)$$

where $\Delta\Phi = \phi_o - \phi_v$ is the azimuth angle difference between the satellite and the sun, and θ_v is the viewing zenith angle.

Each vector, whose components correspond to the SeaWiFS wavelengths, represents a ρ_{used} spectrum.

2.2 The Learning Data Set

The learning data set consists of observed ρ_{used}^{obs} extracted from pixels of SeaWiFS images off the West Africa coast during the year 2003 and two associated viewing angles (i.e., the sun zenith angle θ_s and the scattering angle γ). All the available daily SeaWiFS images were homogeneously sampled (one pixel-line over 10) providing 426,117 clear-sky spectra of ρ_{used}^{obs}. The learning dataset $Data^{obs}$ is thus composed of ten component vectors i.e. the eight wavelengths measured by the radiometer and the two viewing angles.

2.3 The Labeling Data Set

The second data set, $Data^{expert}$ consists of the ρ_{used}^{expert} computed at eight wavelengths with a 2-layer radiative transfer model (Gordon & Wang, 1994) for various optical thickness values, chlorophyll content and geometry of the measurement and for five aerosol models. Each $Data^{expert}$ vector comprises eight spectral components (ρ_{used}^{expert}) and two geometry components which are the sun zenith angle θ_s and the scattering angle γ. To these ten components which were used for the labeling the referent vectors provided by the unsupervised classification, we added the aerosol type and the optical thickness τ at 865 nm. $Data^{expert}$ comprises 6,000,000 simulated vectors using four aerosol models and one absorbing aerosol *(Moulin et al, 2001)*. The five aerosol models were computed at four different relative humidity (70%, 80%, 90%, 99%). $Data^{expert}$ was used in order to introduce the expertise and to retrieve the aerosol type and the optical thickness values.

3 THE METHOD

In this study, we used two successive statistical models for analyzing the $Data^{obs}$ images; the Self Organizing Map (SOM, Kohonen, 2001) model and the NeuroVaria method (Jamet et al., 2005); (Brajard et al., 2006). We first processed the images with a SOM model, which is well suited for visualizing and clustering a high-dimensional data set. We denoted this topological map as SOM-A-S (SOM-Angle-Spectrum). In the light of the results obtained by Niang et al., (2006), we chose a similar architecture for SOM-A-S: a two-dimensional array with a large number of neurons (20 x 30 = 600). SOM-A-S was learned on the $Data^{obs}$ of the year 2003. The vectors of the learning data set were thus clustered into 600 groups, allowing a highly discriminative

representation of $Data^{obs}$. The second dataset, $Data^{expert}$, representing the expertise, was used to decode the SeaWiFS images. The principle of the method is to compare the ten-component vectors of $Data^{expert}$ whose associated parameters are known, with those of the neurons of SOM-A-S according to a distance. At the end of the labeling, each neuron of SOM-A-S map has captured a set of ρ^{expert} and takes a label, which is extracted from that set according to the procedure described in *Niang et al.,* (2006). The only difference between the two versions being that the old one uses a first map to determine 10 different classes of angles, each one giving rise to a dedicated SOM map for the classification of the reflectance spectra, while SOM-A-S uses a unique map doing a data fusion between the viewing angles and the spectra. By using a unique map, we avoided the threshold effect that is induced by the two steps classification (angle and then reflectance) and the eleven SOM maps described in Niang et al., (2003).

Each neuron is therefore associated with an atmospheric and ocean physical parameters (τ, C) and an aerosol type. The SOM-A-S map being labelled, we are able to analyze a satellite image by projecting the ten component vector (reflectances and viewing angles) associated with each pixel on the SOM-A-S map. Pixels captured by a neuron are assigned to the aerosol type and optical thickness associated with this neuron. For monthly climatology images, the aerosol type is estimated as the median of the types of the images considered.

The second statistical model improves the retrieval of the optical thickness. We used a neuro-variational algorithm, called NeuroVaria, that is able to provide accurate atmospheric corrections for inverting satellite ocean-colour measurements. The algorithm minimizes a weighted quadratic cost function, $\boldsymbol{J}$, by adjusting control parameters (atmospheric and oceanic) such as τ and C (Brajard et al., 2008). $\boldsymbol{J}$ describes the difference between the satellite measurement ρ^{obs} and a simulated reflectance ρ^{sim} computed using radiative transfer codes modelled by supervised neural networks (the so called Multi-Layer-Perceptrons, MLP). The minimization implies the computation of the gradient of J with respect to the control parameters and consequently of the derivatives of the MLPs, which is done by the classical gradient back-propagation algorithm (Bishop, 1995). The novelty of the version of NeuroVaria developed in this work is that the MLPs modelling the radiative transfer codes were specially designed to take African dusts into account. Moreover we used the atmospheric parameter values given by SOM-A-S and validated using in situ data (see section 4), as first guesses of the NeuroVaria algorithm minimization. Since the efficiency of a minimizing procedure depends on the first guesses of the control parameters, we expect to improve the accuracy of the retrieved parameters.

Using these two statistical models sequentially is indeed a mixed neuro variational method. We denoted it in the following by SOM-NV.

4 VALIDATIONS OF THE AEROSOL PARAMETERS USING SOM-A-S

As SOM-A-S takes into account Saharan dusts, the number of pixels processed is an order of magnitude higher than that processed by the standard SeaWiFS algorithm. As an example, on October 07 2003, SOM-A-S processed 29,083 pixels while SeaWiFS processed 16,193 pixels only; on October 12 SOM-A-S processed 30,300 pixels and SeaWiFS 3,338 only. Besides a statistical comparison between the SOM-A-S and SeaWiFS algorithms was made for values of τ <0.35. The Mean Relative Error (MRE) remains low (22.88% for October 07 2003 and 16.16% for October 12 2003) and the Root Mean Square Error (RMSE) was less than 0.04 for both days. As a preliminary conclusion, the values retrieved by SOM-A-S seem consistent with and very close to those retrieved by the classical algorithm of SeaWiFS for τ <0.35.

The Angström exponent α(500,870) provided by *AERONET*, allows us to attempt to validate the dust aerosol type provided by SOM-A-S. Since the sun photometer does not give the aerosol type, it is thought possible to validate the dusts by studying the behavior of α (500,870). The low α (500,870) values (α<0.5) result from the presence of large particles typical of desert dusts (Nobileau et al., 2005). In Figure 1 we show the distribution of the α(500,870) of the Dakar-M'Bour *AERONET* measurements for the dusty and the non-dusty days determined by SOM-A-S on the SeaWiFs collocated pixels. The confidence interval of the average value of α (500,870) calculated by SOM-A-S from SeaWiFs measurements for the dusty days was between 0.40 and 0.47, whereas it was between 0.61-0.79 for non-dusty days. This means that the dust classification provided by SOM-A-S is in agreement with the AERONET measurements, which permits us to distinguish the dust absorbing-aerosols from the non-absorbing ones by processing

the SeaWiFs observations with SOM-A-S.

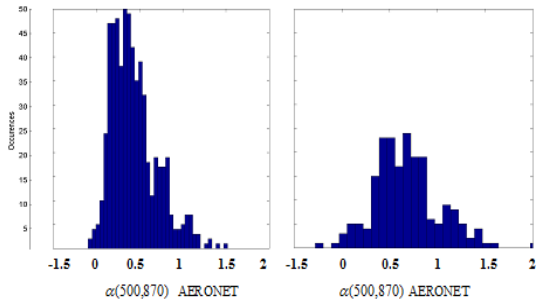

Figure 1: Comparison of the α(500, 870) values measured at the Dakar *AERONET* station for dusty days (left) and for non-dusty days (right). For dusty days, most of the α(500, 870) values are less than 0.5.

5 IMPROVING ATMOSPHERIC RESTITUTION WITH SOM-NV

We processed the 13 year data set of SeaWiFS imagery with SOM-NV. This data set presents a well-marked seasonal variability. Figure 2 shows, as an example, the monthly situations during winter (January), spring (March), summer (July) and autumn (November) of the year 2006 decoded with SOM-NV for the aerosol optical thickness and with SOM-A-S for the aerosol type. In winter (January), the northern part of the studied domain was free of dusts and the optical thickness was almost zero; in the southern part, we observed the presence of Saharan dusts with a small concentration (small optical thickness). In spring, the Saharan dusts moved northward and their concentration (optical thickness) increased. In summer, the Saharan dusts invaded the entire domain and their concentration was maximal. In autumn, the Saharan dusts disappeared but we noted a low optical thickness in the whole domain due to the presence of non-absorbing aerosols. The year 2006 represents a typical year of the data set concerning the seasonal variability, which is observed every year.

During winter, spring and summer, the presence of Saharan dusts is linked to the westward wind, eroding the Sahara ground and transporting dusts over the Atlantic, as seen in Figure 2. The extent of Saharan dust is maximal in summer when the Inter Tropical Convergence Zone (ITCZ) is at its maximum latitude. The situation in autumn is puzzling. The wind is still blowing westward in the southern part of the domain but we do not detect any Saharan dust. A possible explanation might be due to the fact that in autumn, the vegetation has developed following the summer rain, (summer is the rainy season). The vegetation and soil humidity inhibit the erosion of the ground in the southern region of the Sahara, which might explain the absence of dust south of 20°N in autumn.

A validation can therefore be made by comparing the optical thickness values retrieved by SOM-NV and the SeaWiFS algorithm and those measured at the *AERONET* stations of Dakar and Cabo Verde, respectively denoted $\tau^{SOM\text{-}NV}$, $\tau^{SeaWiFS}$ and τ^{AERO}.

We determine τ, by taking the mean value of the five SeaWiFS measurements surrounding the AERONET ground stations.

We ended up, at the two ground stations, with 1,288 measurements collocated for SOM-NV retrievals and 623 measurements collocated for the standard SeaWiFS algorithm (fewer because of the dust mask). We compared the RMSE and the MRE of $\tau^{SOM\text{-}NV}$ and $\tau^{SeaWiFS}$ with respect to the observed τ^{AERO}.

The results for the *AERONET* measurements collocated with those of SeaWiFS and the SOM-NV for which the SeaWiFS optical thickness value was less than 0.35 (SeaWiFS critical value) are presented in Table 1. Table 2 shows comparisons for the *AERONET* measurements collocated with those of the available SOM-NV, which only include measurements for which the optical thickness value was higher than 0.35.

The correlation coefficient between $\tau^{SOM\text{-}NV}$ and τ^{AERO} is higher than that between $\tau^{SeaWiFS}$ and τ^{AERO} showing the good performances of the SOM-NV method. This is confirmed by the scatter plot of $\tau^{SOM\text{-}NV}$ and τ^{AERO}, and τ^{SeaW} and τ^{AERO} (Figure 3 for Dakar, Figure 4 for Cabo Verde). But it is also important to note that the SOM-NV neural decoding allows the retrieval of high optical thickness values (i.e., greater than 0.35, above which the SeaWiFS algorithm does not work) with a good accuracy.

6 CONCLUSIONS

We have developed an original and efficient two-step method for retrieving optical properties (type and optical thickness) from TOA reflectance measured by satellite-borne multi-spectral ocean-color sensors. The method is based on a combination of a neural network classification and a variational optimization. It makes use of the full spectrum and two viewing angles of measurements to perform the aerosol identification.

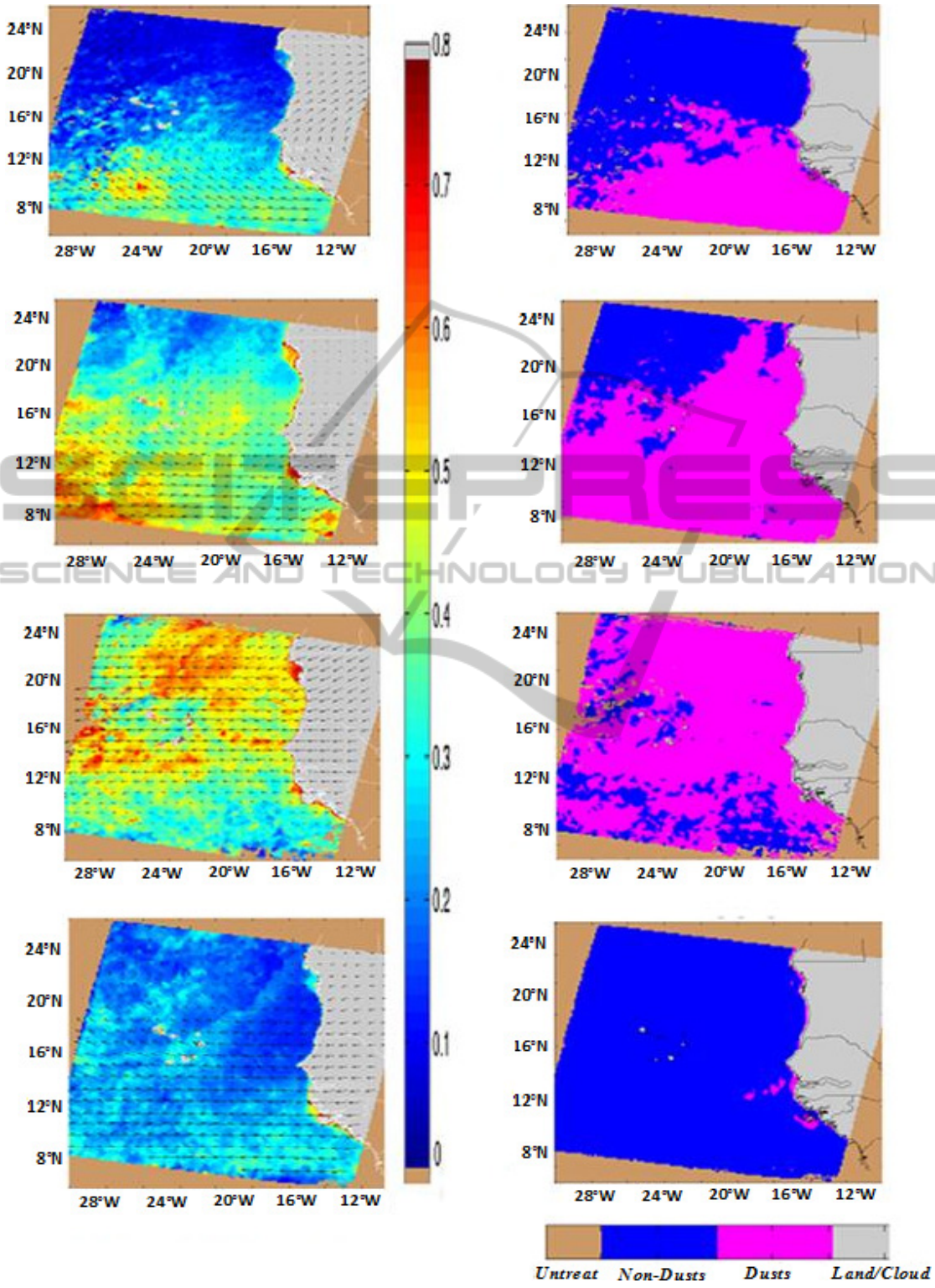

Figure 2: Monthly map of optical thickness (left panels) computed with SOM-NV and extent of Saharan dust (right panels) for (from top to bottom) January, March, July and November 2006 computed with SOM-A-S.

SCITEPRESS
SCIENCE AND TECHNOLOGY PUBLICATIONS

Table 1: Comparison of the performances (RMSE and MRE) obtained on the optical thickness (< 0.35) computed by the SOM-NV and the SeaWiFS product with respect to the concomitant AERONET measurements at Dakar (M'Bour) and Cabo Verde (Sal Island) averaged for the 12 years from 1997 to 2009.

Station	Number of Collocated data	RMSE		MRE (%)		Correlation coefficient	
		SOM-NV	SeaW.	SOM-NV	SeaW.	SOM-NV	SeaW.
Dakar	232	0.023	0.025	33.8	32.6	0.83	0.69
Cap-Vert	391	0.017	0.018	42.2	40.8	0.79	0.70

Table 2: Performances (RMSE and MRE) obtained on the optical thickness computed by the SOM-NV for τ >0.35 only, with respect to AERONET measurements at Dakar (M'Bour) and Cabo Verde averaged for the 12 years.

Station	Number of Collocated data	RMSE	MRE (%)	Correlation coefficient
Dakar	338	0.025	21.9	0.88
Cap-Vert	327	0.024	25.2	0.91

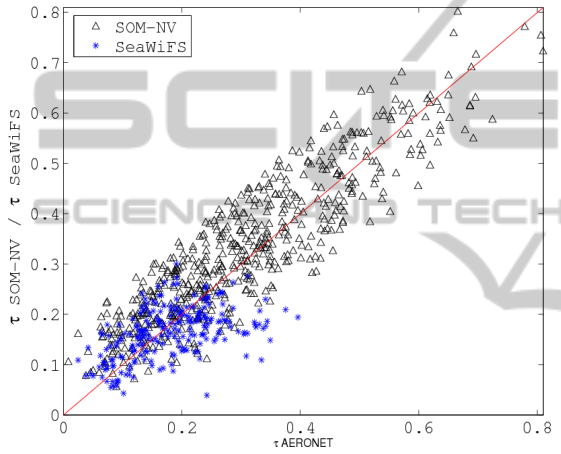

Figure 3: Scatter plot of the optical thickness measurements computed by SOM-NV (Δ) and the SeaWiFS product (*) with respect to the AERONET measurements at Dakar.

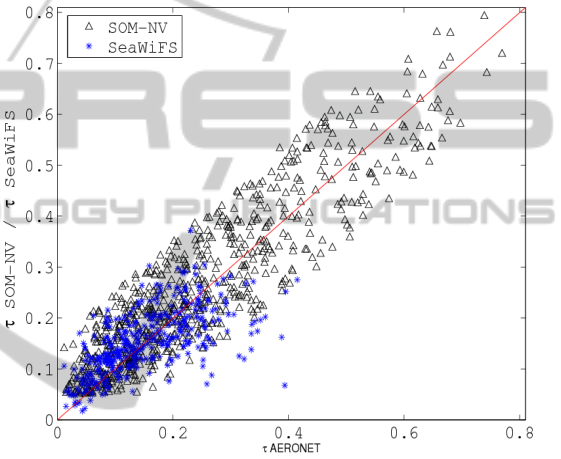

Figure 4: Scatter plot of the optical thickness measurements computed by SOM-NV (Δ) and the SeaWiFS product (*) with respect to the AERONET measurements at Cabo Verde.

This new method allows retrieval of the aerosol optical properties from the statistical properties of the data and for the first time the identification of the aerosol type. Besides, it gives accurate results for optical thickness values greater than 0.35, which is not the case for the standard SeaWiFS product. This allowed us to substantially increase the number of pixels processed with respect to the standard SeaWiFS algorithm by an order of magnitude as shown in Table 1 and Table 2. Moreover, the method permits detection of absorbing aerosols, such as Saharan dusts, which is still a challenge.

The monthly mean optical thickness measured by the SeaWiFS sensor is strongly correlated with the ground based measurements (AERONET stations), which validates the pertinence of the method. Analysis of the 13 years of observation show an important seasonal variability associated with the wind direction and intensity. The Saharan dust concentration is maximal in summer when the ITCZ is at its maximum latitude and minimum in autumn when the vegetation bloom reduces the soil erosion by the wind. This 13 year climatological data set available at http://www.locean-ipsl.upmc.fr/~POACC/ may be used to assess the seasonal variability of the mass of Saharan dust transported by the wind over the Atlantic Ocean. This new method can be easily implemented. Climatologists will get a better estimate of the aerosol concentration over the ocean and will have access to the aerosol type, which is important to understand their impact on climate.

ACKNOWLEDGEMENTS

We are grateful for the support we received from CNES and IRD. We thank Dr. H. R. Gordon and C.

Moulin for providing the synthetic database. We thank the AERONET team and Dr. Tanré from LOA (Lille) for kindly providing the sun-photometer data at Dakar and Cabo Verde.

REFERENCES

Bishop, C. (1995). Neural networks for pattern recognition. *Oxford University Press.*

Brajard, J., Jamet, C., Moulin, C. and Thiria, S. (2006). Use of a neuro-variational inversion for retrieving oceanic and atmospheric constituents from satellite ocean colour sensor: Application to absorbing aerosols. *Neural Networks 19, 178-185.*

Brajard, J., Niang, A., Sawadogo, S., Fell, F., Santer, R and Thiria, S. (2007). Estimating Aerosol parameters from MERIS ocean colour sensor observations by using topological maps. *Intern. J. Remote Sensing , Vol28, N° 3-4 pp 781-795.*

Gordon, H. R. & Wang, M. (1994). Retrieval of water-leaving radiances and aerosol optical thickness over the oceans with SeaWiFS: A preliminary algorithm. *Applied Optics, 33(3), 443-453.*

Holben, B., Eck, T., Slutsker, I., Tanré, D., Buis, J. P., Setzer, A., et al. (1998). AERONET. A federated instrument network and data archive for aerosol characterization. *Remote Sensing of Environment, Vol. 66, n°1, p. 1-16.*

Husar, R., Stowe, L. and Prospero, J. (1997). Characterization of tropospheric aerosols over the oceans with NOAA advanced very high resolution radiometer optical thickness operational product. *Journal of Geophysical Research, 102(16), 889-909.*

Jamet, C., Thiria, S., Moulin, C., and Crepon, M. (2005). Use of a neuro-variational inversio for retrieving oceanic and atmospheric constituents from ocean color imagery. A feasibility study. *Journal of Atmospheric and Oceanic Technology, 22(4), 460-475. Doi:10.1175/JTECH1688.1*

Kohonen, T. (2001). Self organizing maps (3rd ed.). *Berlin Heidelberg: Springer Verlag. p. 501.* Moulin, C., Lambert, C. E., Dulac, F. and Dayan, U. (1997). Control of atmospheric export of dust from North Africa by the North Atlantic Oscillation. *Nature, 387, 691-694.*

Moulin, C., Gordon, H. R., Banzon, V. F., and Evans, R. H. (2001). Assessment of Saharian dust absorption in the visible from SeaWiFS imagery. *Journal of Geophysical Research, 106, 18239-18250.*

Niang, A., Badran, F., Moulin, C., Crépon, M. & Thiria, S. (2006). Retrivial of aérosol type and optical thickness over the Mediterranean from SeaWiFS images using an automatic neural classification method. *Remote Sensing of Environment, Vol. 100, n°1, p. 82-94.*

Nobileau, D. and Antoine, D. (2005). Detection of blue-absorbing aerosols using near-infrared and visible (ocean color) remote sensing observations. *Remote Sensing of Environment, Vol. 95, n°3, p. 368-387.*

Tanre, D., Deroo, C., Duhaut, P., Herman, M., Morcrette, J., Perbos, J. and Deschamps, P. Y. (1997). Description of a computer code to simulate the satellite signal in the solar spectrum: 5s code. *International Journal of Remote Sensing, 11 : 659-668.*

SCITEPRESS SCIENCE AND TECHNOLOGY PUBLICATIONS